Robust MEG Source Localization of Event Related Potentials: Identifying Relevant Sources by Non-Gaussianity

Peter Breun[1], Moritz Grosse-Wentrup[2], Wolfgang Utschick[1], and Martin Buss[2]

[1] Institute for Circuit Theory and Signal Processing, Technische Universität München, 80290 München, Germany
breun@nws.ei.tum.de, utschick@tum.de

[2] Institute of Automatic Control Engineering (LSR), Technische Universität München, 80290 München, Germany
moritz@tum.de, mb@tum.de

Abstract. Independent Component Analysis (ICA) is a frequently used preprocessing step in source localization of MEG and EEG data. By decomposing the measured data into maximally independent components (ICs), estimates of the time course and the topographies of neural sources are obtained. In this paper, we show that when using estimated source topographies for localization, correlations between neural sources introduce an error into the obtained source locations. This error can be avoided by reprojecting ICs onto the observation space, but requires the identification of relevant ICs. For Event Related Potentials (ERPs), we identify relevant ICs by estimating their non-Gaussianity. The efficacy of the approach is tested on auditory evoked potentials (AEPs) recorded by MEG. It is shown that ten trials are sufficient for reconstructing all important characteristics of the AEP, and source localization of the reconstructed ERP yields the same focus of activity as the average of 250 trials.

1 Introduction

Event related potentials (ERPs) are magnetic/electric fields of the brain elicited by an event such as presentation of a visual or an auditory stimulus. These fields can be measured outside the skull using magneto- or electroencephalography (MEG/EEG). While all concepts presented in this paper can be applied equally to MEG or EEG, we restrict our discussion to MEG for the sake of simplicity. In the study of ERPs, the process of source localization is concerned with determining the position of neural generators causing the ERP, which allows conclusions about brain areas involved in processing a stimulus. A wide range of methods has been developed for MEG source localization, ranging from simple dipole to distributed source models (see [1] for a review). Common to all methods is their susceptibility to noise, requiring a high signal-to-noise ratio (SNR) of the ERP.

ERPs, however, are cloaked by ongoing background MEG activity usually several times the magnitude of the signal of interest. To extract ERPs from the magnetic background activity numerous trials are recorded, in which the stimulus

K. Franke et al. (Eds.): DAGM 2006, LNCS 4174, pp. 394–403, 2006.

is presented repeatedly to the subject. Under the assumption that only the ERP component of the magnetic field is invariant for every stimulus presentation, the average time course of all trials results in an unbiased estimate of the original ERP. The computation of this so called *grand average* ERP usually requires several hundred trials if a positive SNR is desired. Since this amount of data is not always available, source localization algorithms may perform poorly, rendering these approaches impractical for a large group of experimental setups.

For these reasons, the development of methods for source localization that are insensitive to MEG background activity is an active area of research. In this paper, we focus on using Independent Component Analysis (ICA) for this purpose. ICA is a special case of Blind Source Separation (BSS), that decomposes the measured data into maximally independent components (ICs) [2]. In the context of source localization, ICA is used as a preprocessing step to obtain estimates of the topographies of neural sources. The position of a source inside the brain can then be estimated from its topography without interference from other neural sources [3,4]. This approach introduces an error into the localization process if the neural sources are not fully statistically independent. As a remedy, we show that reprojection of the relevant ICs onto the observation space, and subsequent source localization of the reprojected data, removes this error. This approach requires identification of the ICs contributing to the ERP. This can be done by estimating the non-Gaussianity of each IC.

The efficacy of our approach is tested on auditory evoked potentials (AEPs) recorded by MEG. Ten trials are randomly chosen from a total of 250 trials. Using ICA and reprojecting the most non-Gaussian IC onto the observation space is shown to result in a SNR of 5.52 dB in comparison to the grand average of 250 trials. Reconstructing the current density with a distributed source model results in identical maxima of current strength for the ERP reconstructed from ten trials and the grand average ERP of 250 trials.

The rest of this paper is organized as follows. We first introduce the source model, followed by a review of source localization using distributed source models and ICA. We will then show why correlations between neural sources introduce an error into the source localization procedure when using source topographies estimated by ICA. This motivates the reprojection of relevant ICs onto the observation space, which renders the localization procedure more robust to source correlations. The relevant ICs contributing to the ERP are then identified by estimating their non-Gaussianity. In the results section, we apply the proposed procedure to AEPs recorded by MEG, and conclude with a brief discussion.

2 Methods

2.1 Source Model

The determination of the current density from MEG measurements is an ill-posed problem which has no unique solution. A first step to obtain a solution to this inverse problem is to constrain the possible current sources to be dipoles, since the synchronized pre-synaptic potentials of neurons in a cortical column,

that give rise to the MEG, can be approximated by a single current dipole [1]. We restrict ourselves to a spherical head model which allows for a simple determination of the magnetic field $\boldsymbol{y}_k$ at the sensor positions generated by the k-th dipole with known location and orientation (forward problem) [5]:

$$\boldsymbol{y}_k = \boldsymbol{A}_k \boldsymbol{s}_k \in \mathbb{R}^M, \tag{1}$$

with the leadfield matrix $\boldsymbol{A}_k \in \mathbb{R}^{M\times 3}$ of dipole k where M is the number of available MEG sensors and $\boldsymbol{s}_k = [s_{k,x}, s_{k,y}, s_{k,z}]^{\mathrm{T}}$ contains the dipole moment in x, y and z direction.[1] The magnetic field generated by N dipoles is the superposition of $\boldsymbol{y}_k, k = 1, \ldots, N$. Thus, the model to be used in the sequel is

$$\boldsymbol{y} = \boldsymbol{A}\boldsymbol{s}, \tag{2}$$

with $\boldsymbol{A} = [\boldsymbol{A}_1, \ldots, \boldsymbol{A}_N] \in \mathbb{R}^{M\times 3N}$ and $\boldsymbol{s} = [\boldsymbol{s}_1^{\mathrm{T}}, \ldots, \boldsymbol{s}_N^{\mathrm{T}}]^{\mathrm{T}} \in \mathbb{R}^{3N}$. The measurement noise is neglected.

Note that the moment vector $\boldsymbol{s}_k \in \mathbb{R}^3$ can be written as $\frac{\boldsymbol{s}_k}{\|\boldsymbol{s}_k\|_2}\|\boldsymbol{s}_k\|_2 = \boldsymbol{p}_k m_k$, with the unit norm moment orientation vector $\boldsymbol{p}_k \in \mathbb{R}^3$ and the scalar dipole moment m_k. If the orientation vectors are known or can be estimated simultaneously with the matrix $\boldsymbol{A}$, (2) becomes

$$\boldsymbol{y} = \boldsymbol{G}\boldsymbol{m}, \tag{3}$$

with $\boldsymbol{m} = [m_1, \ldots, m_N]^{\mathrm{T}}$ and $\boldsymbol{g}_k = \boldsymbol{A}_k \boldsymbol{p}_k$, where $\boldsymbol{g}_k$ is the k-th column of $\boldsymbol{G} \in \mathbb{R}^{M\times N}$.

2.2 Source Localization

Because of the complex mathematical structure of spatially unconstrained dipole fitting [1], we estimate a discrete approximation of the current density using a large number of current dipoles, placed on a regular grid. It remains to determine the contribution of each of these fixed dipoles to the measurement, thereby reducing the localization to a linear inverse problem ("distributed linear" or "imaging" methods [1]). Because there are typically much more dipoles than sensors, this approach leads to an underdetermined system of linear equations. In order to find a unique solution, it has to be regularized, usually by incorporating assumptions about the spatial properties of the solution, e. g., the norm [6], smoothness [7] or sparseness [8]. These algorithms often use one measurement in time, but there are also attempts to include the temporal evolution (e. g., [9]).

In this paper, we use a distributed approach to determine strongly localized solutions to the inverse problem.[2] Thus, we impose the constraint for the solution to be sparse. This is achieved by the following optimization [10]:

$$\min_{\boldsymbol{s}} \|\boldsymbol{A}\boldsymbol{s} - \boldsymbol{y}\|_2 + \lambda \|\boldsymbol{s}\|_1 . \tag{4}$$

[1] Note that for MEG the matrix $\boldsymbol{A}_k$ has rank 2, since radial dipoles do not contribute to the measurements [5]. Therefore, the dimension of the model could be reduced.

[2] This spatial assumption might not be valid for all neural sources (e. g. cognitive processes) but applies to the AEPs investigated in the results section.

The leadfield matrix $\boldsymbol{A}$ is known here because it is fully determined by the fixed positions of the dipoles on the grid. The first term of (4) is used to find a solution which gives a good approximation of the measured data. The second term penalizes the ℓ_1 norm of the solution vector which is known to produce sparse solutions [10]. The regularization parameter λ trades the data approximation with the degree of sparsity. Note that this optimization would lead to a solution that is not only sparse in the overall dipole moment, but also in its x, y and z components which has no physiological justification. Thus, a modified penalty on the norm (see, e. g., [9]) of the solution vector is introduced:[3]

$$\|\boldsymbol{s}\|_{2,1} \triangleq \sum_{n=1}^{N} \|\boldsymbol{s}_n\|_2 = \sum_{n=1}^{N} \left| \left(\sum_{k\in\{x,y,z\}} s_{n,k}^2 \right)^{\frac{1}{2}} \right|. \tag{5}$$

This produces a sparse solution in the overall dipole moments but not in the respective moment components since the ℓ_2 norm is not sparsity enforcing. The resulting optimization problem

$$\min_{\boldsymbol{s}} \|\boldsymbol{A}\boldsymbol{s} - \boldsymbol{y}\|_2 + \lambda \|\boldsymbol{s}\|_{2,1} \tag{6}$$

is a second order cone program and can be solved efficiently using standard numerical optimization tools.

2.3 Independent Component Analysis

More recently, it has been proposed to apply ICA [2] to perform a BSS of the dipole sources using the measurements of their superimposed activity [11]. This approach explicitly uses the fact that typically not only one MEG measurement is available, but a whole (sampled) time course, and decomposes the measured signal into statistically maximally independent components.

In order to get interpretable results from the ICA, we make the following *assumptions*: The time courses of the dipole moments of ERPs are non-Gaussian distributed and statistically independent to the non-event related background brain activity. This enables us to identify and separate sources as ICs contributing to the ERPs. Furthermore, we assume that there is only a small number $L < N$ of sources with non-Gaussian dipole moment. This assumption is based on the observation that only a few ICs can be consistently reconstructed, which implies that the other sources have a Gaussian distribution [12]. Additionally—for ICA, not for the subsequent source localization—we restrict ourselves to the case of $N \leq M$, i. e., at least as many sensors as sources. If less sources than sensors are present, a Principal Component Analysis (PCA) of the data with a projection on the signal subspace can be performed [13]. Referring to the model introduced in (3), we have T measurements

$$\boldsymbol{y}[t] = \boldsymbol{G}\boldsymbol{m}[t], \quad t \in \{1, 2, \ldots, T\}, \tag{7}$$

[3] Note that the absolute value in (5) is not necessary. It is included to emphasize the application of the ℓ_1 norm to the Eucledian (ℓ_2) norms of $\boldsymbol{s}_n$, $n \in \{1, 2, \ldots N\}$.

where it is assumed that the matrix $\boldsymbol{G}$ and thus the location and orientation of the source dipoles do not change over time.

In order to perform a BSS, we determine a so called unmixing matrix $\boldsymbol{W}$ such that, applied to the measurements $\boldsymbol{y}[t]$, the components of the resulting vector are statistically independent. For the quadratic case ($M = N$), $\boldsymbol{W}$ is an estimate of the inverse of $\boldsymbol{G}$:[4]

$$\hat{\boldsymbol{m}}[t] = \boldsymbol{W}\boldsymbol{y}[t] = \boldsymbol{W}\boldsymbol{G}\boldsymbol{m}[t] = \boldsymbol{P}\boldsymbol{m}[t]. \tag{8}$$

This matrix can be found by minimizing the mutual information between the components of the vector $\hat{\boldsymbol{m}}[t]$, the ICs:

$$\min_{\boldsymbol{W}} I\left(\hat{m}_1, \ldots, \hat{m}_N\right) = \sum_{n=1}^{N} H\left(\hat{m}_n\right) - H\left(\hat{\boldsymbol{m}}\right) \text{ s.t. } \|\boldsymbol{w}_n\|_2 = 1,\ n \in \{1, \ldots, N\}, \tag{9}$$

with the differential entropy $H(z) = -\int_{-\infty}^{\infty} p_z(u) \log\left(p_z(u)\right) \mathrm{d}u$ [14,15]. Note that only the L non-Gaussian sources can consistently be found by this method, the remaining $N - L$ Gaussian sources are arbitrarily mixed together [12]. An estimate of the leadfield matrix $\boldsymbol{G}$ is obtained by inverting $\boldsymbol{W}$, i. e., $\hat{\boldsymbol{G}} = \boldsymbol{W}^{-1}$.

2.4 ICA for Source Localization

In the previous section, a method has been described to obtain an estimate $\hat{\boldsymbol{G}}$ of the leadfield matrix and the ICs. In [4], the assumption that each IC corresponds to a single dipole and all sources have mutually independent time courses allowed for a decoupled dipole fit since the k-th column $\hat{\boldsymbol{g}}_k$ of $\hat{\boldsymbol{G}}$, also called the topography of the k-th IC, only depends on the parameters of dipole k. If one assumes that $\hat{\boldsymbol{g}}_k$ corresponds to a distributed source rather than a single dipole, a decoupled localization based on (6) is possible:[5]

$$\min_{\boldsymbol{s}} \|\boldsymbol{A}\boldsymbol{s} - \hat{\boldsymbol{g}}_k\|_2 + \lambda \|\boldsymbol{s}\|_{2,1}, \qquad k \in \{1, \ldots, N\}. \tag{10}$$

A problem arises if the assumption of mutually independent sources contributing to the ERP is violated. Suppose a model with two sources which are obtained by a linear transformation from two statistically independent and non-Gaussian sources $\boldsymbol{m}' \in \mathbb{R}^2$:

$$\boldsymbol{m} = \boldsymbol{T}\boldsymbol{m}' \in \mathbb{R}^2. \tag{11}$$

This gives the observation

$$\boldsymbol{y} = \boldsymbol{G}\boldsymbol{m} = \boldsymbol{G}\boldsymbol{T}\boldsymbol{m}' = \boldsymbol{G}'\boldsymbol{m}', \tag{12}$$

[4] Note that $\boldsymbol{W}\boldsymbol{G}$ is not the identity but the product $\boldsymbol{P}$ of a permutation and diagonal matrix due to the insensivity of the cost function (9) w. r. t. this operation.

[5] The column $\hat{\boldsymbol{g}}_k$ is not multiplied with the corresponding IC $\hat{m}_k$ since this changes the minimizer of (10) only by a scalar factor.

with $\boldsymbol{G}' = \boldsymbol{G}\boldsymbol{T}$. The effective mixing matrix $\boldsymbol{G}'$ can now be identified by ICA.[6] Assuming the transformation

$$\boldsymbol{T} = \begin{bmatrix} 1 & c \\ c & 1 \end{bmatrix}, \qquad c \in \mathbb{R}, \tag{13}$$

the correlation of the components of $\boldsymbol{m}$ is determined by the scalar c and the two columns of the matrix $\boldsymbol{G}'$, read as $\boldsymbol{g}'_1 = \boldsymbol{g}_1 + c\boldsymbol{g}_2$ and $\boldsymbol{g}'_2 = c\boldsymbol{g}_1 + \boldsymbol{g}_2$. As long as $|c| \neq 1$, these two columns are linearly independent and can be identified by ICA. However, the columns $\boldsymbol{g}'_1$ and $\boldsymbol{g}'_2$ are not identical to $\boldsymbol{g}_1$ and $\boldsymbol{g}_2$, and thus an error is introduced if they are used for a decoupled source localization (see 10). The effect on source localization demonstrated by this simple example might not be a problem if (10) is used, since only linear correlations are present. However, it is emphasized that care should be taken if the independence assumption does not hold in general. This phenomenon can occur, e. g., for the case of AEPs [16]. In the next subsection, we propose a method to deal with this problem.

2.5 ICA for Preprocessing of MEG Data

While the results of ICA may not be directly suitable for a source localization, they can still be used to extract relevant activity from the measured data. This "denoised" signal can then be the basis for a more accurate localization.

A major assumption of the presented ICA approach is that only neural activity of interest results in a non-Gaussian signal, while the Gaussian background activity results in Gaussian ICs. This gives a criterion to decide which components contribute to the signal of interest. Assuming that there are L non-Gaussian ICs, we get a "denoised" signal by computing

$$\hat{\boldsymbol{y}}[t] = \hat{\boldsymbol{G}}^{(L)} \hat{\boldsymbol{m}}^{(L)}[t], \tag{14}$$

where $\hat{\boldsymbol{m}}^{(L)}[t] \in \mathbb{R}^L$ contains only the non-Gaussian ICs and $\hat{\boldsymbol{G}}^{(L)} \in \mathbb{R}^{M \times L}$ the corresponding columns of $\boldsymbol{W}^{-1}$.[7] For the estimation of Gaussianity, we employ the Anderson-Darling test (see, e. g., [17]) which is based on a distance measure between the empirical distribution function of the available data and the cumulative distribution function to be tested for. This is done separately for each IC, since they are assumed to be statistically independent.

The advantage of this approach lies in the fact that the columns of $\hat{\boldsymbol{G}}$, which may be affected by correlations of the signal components, are not used for a decoupled source localization. Instead, we remove the signal portion assumed to be background activity that is statistically independent to the signal of interest and proceed with a simultaneous localization of the remaining sources. Assuming that the non-Gaussian ICs have been correctly identified, the signal $\hat{\boldsymbol{y}}[t]$ is used as data for the source localization algorithm as described above.

[6] Up to permutation and scaling which is not considered here for simplicity.

[7] Note $\boldsymbol{W}^{-1}$ is actually an estimate of $\boldsymbol{G}'$ (with the problems mentioned in Section 2.4). Only for statistically independent sources, this is also an estimate of $\boldsymbol{G}$.

3 Results

To test the efficacy of the proposed approach, we used MEG data recorded during an auditory oddball task at the Biomagnetic Imaging Laboratory at the University of California, San Francisco. The data was collected with $M = 132$ channels covering the right hemisphere, and was sampled at 4 kHz. Each trial started with presentation of an auditory stimulus to the left ear, and lasted 275 ms (see [18] for a description). The grand average ERP $\boldsymbol{y}^*$ was calculated as the average of 250 trials and low-pass filtered with 16 Hz cut-off frequency [15]. The resulting time course at all channels is shown in Fig. 1 (left panel).

Ten trials were chosen randomly as test data. After low-pass filtering with 50 Hz cut-off frequency and subtracting the mean of each channel, a PCA was performed, only retaining the first 50 principal components [13].[8] The extended Infomax-ICA algorithm [14] was applied to the concatenated trials, resulting in 50 ICs and associated topographies $\left\{\hat{m}_k[t], \hat{\boldsymbol{g}}_k \in \mathbb{R}^M\right\}$, $k = 1, \ldots, 50$. After computing the mean time course across the ten trials for each IC, the non-Gaussianity of each averaged IC was estimated using the Anderson-Darling test mentioned in section 2.5.

A remarkable result is that only one IC showed a high degree of non-Gaussianity, which was 5.9 times the standard deviation (std) apart from the mean non-Gaussianity of all ICs. This IC was only ranked eighth in terms of explained variance of the original measurements as expected from the low SNR of the data set. Since the IC with the second highest non-Gaussianity was only 2.4 stds apart from the mean non-Gaussianity, only the most non-Gaussian IC was assumed to contribute to the ERP. Hence, we conclude that $L = 1$.

To reconstruct the ERP, the most non-Gaussian IC was reprojected onto the observation space (cf. 14), and the reconstructed ERP $\hat{\boldsymbol{y}}$ was compared with the grand average ERP $\boldsymbol{y}^*$ by computing the SNR, defined as [18]

$$\mathrm{SNR} = 10 \log_{10} \left[\frac{1}{M} \sum_{i=1}^{M} \left(\sum_{t=1}^{N} y_i^*[t]^2 \right) \Big/ \left(\sum_{t=1}^{N} \left(y_i^*[t] - \hat{y}_i[t] \right)^2 \right) \right] (\mathrm{dB}). \quad (15)$$

This resulted in a SNR of 5.52 dB and the time course shown in the middle panel of Fig. 1. In comparison with only averaging the ten trials and low-pass filtering the resulting raw average with 16 Hz cut-off frequency (Fig. 1, right panel), an increase in SNR of 5.79 dB was achieved.[9]

The effect of the denoising for source localization was assessed by estimating the current distribution for all three data sets (i. e., grand average, reconstructed and average, see Fig. 1), using the distributed source localization procedure described in the methods section. A spherical head model was assumed, with the MEG sensors located at a radius of 8.5 cm. A regular grid with an inner radius

[8] Here, we have to set $M = 50$ for ICA and can therefore reconstruct up to $N = 50$ ICs. Note that M and N have different values for the subsequent source localization.

[9] Note that for comparison the grand average, reconstructed and average only, ERPs were all normalized to their first major peak occurring around 95 ms.

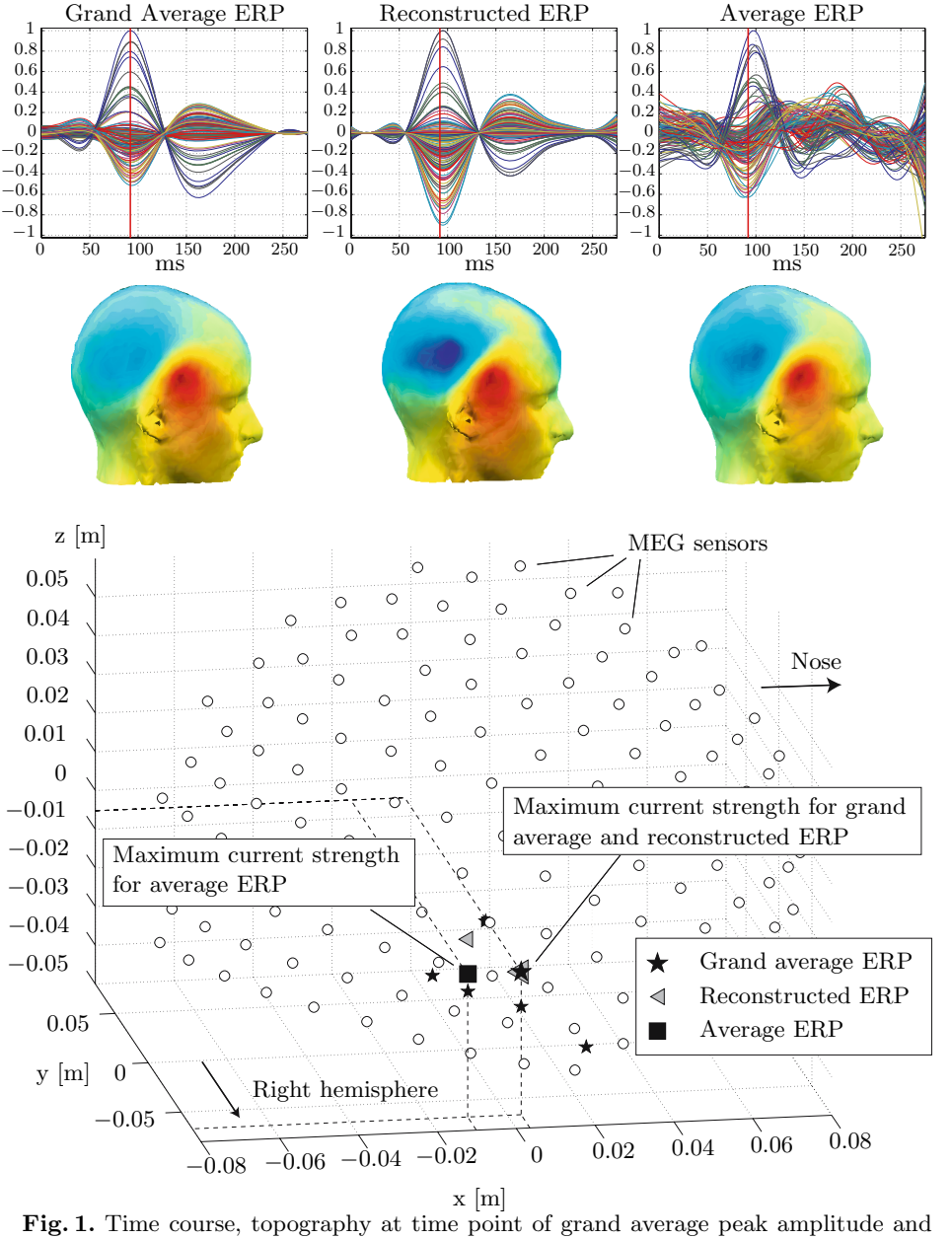

Fig. 1. Time course, topography at time point of grand average peak amplitude and current distribution for grand average, denoised and raw average ERP datasets. The vertical line in the first row shows the time index of the topographies and source localization results in the two lower panels. The topographies were plotted using EEGLab [15].

of 5.5 cm and outer radius of 7.1 cm was placed inside the spherical head model, with a distance of 4.5 mm between each grid point. This resulted in $N = 7437$ dipoles. The time instant of maximum amplitude of the grand average ERP (92 ms) was chosen for localization for all three data sets. The same regularization parameter was used for all data sets, with λ chosen to achieve a good trade-off between sparsity and approximation of the measurements (resulting in a residual variance of 0.73% for the grand average, 7.6% for the reconstructed and 1.9% for the average only ERP). The results of the localization are shown in the bottom row of Fig. 1. The location of maximum current strength for the grand average, the reconstructed and the average ERP are indicated by the major star, triangle and square, respectively. Smaller indicators represent grid points with a current strength of at least 50% of the maximum current strength.

The grid point of maximum current strength of the reconstructed ERP coincided with the maximum grid point of the grand average ERP. The maximum current strength for the average ERP on the other hand was located three grid points (1.35 cm) apart from the focus of activity of the grand average ERP. Five points of the grand average ERP showed a current strength of at least 50% of the maximum current strength, while this was the case for only one more point for the reconstructed ERP.

4 Discussion

To summarize the results, the proposed approach proved capable of achieving a significant increase of SNR in comparison to only averaging and low-pass filtering the data (+5.79 dB). While the peak latencies and amplitudes of the AEP were difficult to identify in the averaged data set, the reconstructed ERP showed a similar time course as the grand average ERP, with all peaks clearly identifiable. We conclude, that with the proposed approach a small number of trials is sufficient to reconstruct the most important characteristics of ERPs. Furthermore, the results support our assumption that non-Gaussianity of ICs is a good criterion for identifying ICs contributing to an ERP.

In terms of source localization, the focus of activity of the reconstructed ERP coincided with the grand average ERP, while the focus of activity of the average ERP was shifted by 1.35 cm. It should be noted that AEPs have a relatively high SNR compared to other ERPs, resulting in acceptable results by averaging only. Further studies have to show, how our approach performs in comparison to only averaging if more complex experimental setups are being investigated.

Finally, it should be noted that the data set used in this study was not well suited for investigating the issue of correlations between neural sources discussed in section 2.4. Since one IC was sufficient to reconstruct the grand average ERP, it can be concluded that no correlations between neural sources contributing to the ERP existed.[10] This issue will also be investigated in further simulation studies and studies with more complex experimental setups.

[10] Note that this does not exclude the possibility of the most non-Gaussian IC representing a distributed source.

References

1. Baillet, S., Mosher, J.C., Leahy, R.M.: Electromagnetic brain mapping. IEEE Signal Processing Magazine **18**(6) (2001) 14–30
2. Comon, P.: Independent component analysis, a new concept? Signal Processing **36**(3) (1994) 287–314
3. Cao, J., Murata, N., Amari, S., Cichocki, A., Takeda, T.: Independent component analysis for unaveraged single-trial MEG data decomposition and single-dipole source localization. Neurocomputing **49** (2002) 255–277
4. Zhukov, L., Weinstein, D., Johnson, C.: Independent component analysis for EEG source localization - an algorithm that reduces the complexity of localizing multiple neural sources. IEEE Engineering in Medicine and Biology Magazine **19**(3) (2000) 87–96
5. Mosher, J.C., Lewis, P.S., Leahy, R.M.: Multiple Dipole Modeling and Localization from Spatio-Temporal MEG Data. IEEE Transactions on Biomedical Engineering **39**(6) (1992) 541–557
6. Hämäläinen, M.S., Ilmoniemi, R.J.: Interpreting magnetic fields of the brain: minimum norm estimates. Medical & Biological Engineering & Computing **32** (1994) 35–42
7. Pascual-Marqui, R.D., Michel, C.M., Lehmann, D.: Low resolution electromagnetic tomography: a new method for localizing electrical activity in the brain. International Journal of Psychophysiology **18** (1994) 49–65
8. Gorodnitsky, I.F., George, J.S., Rao, B.D.: Neuromagnetic source imaging with FOCUSS: a recursive weighted minimum norm algorithm. Journal on Electroencephalography and clinical Neurophysiology **95**(4) (1995) 231–251
9. Cotter, S.F., Rao, B.D., Engan, K., Kreutz-Delgado, K.: Sparse Solutions to Linear Inverse Problems With Multiple Measurement Vectors. IEEE Transactions on Signal Processing **53**(7) (2005) 2477–2488
10. Chen, S.S., Donoho, D.L., Saunders, M.A.: Atomic decomposition by basis pursuit. SIAM Journal on Scientific Computing **20**(1) (1998) 33–61
11. Makeig, S., Bell, A.J., Jung, T.P., Sejnowski, T.J.: Independent Component Analysis of Electroencephalographic Data. In Touretzky, D.S., Mozer, M.C., Hasselmo, M.E., eds.: Advances in Neural Information Processing Systems 8, MIT Press (1996) 145–151
12. Grosse-Wentrup, M., Buss, M.: Subspace Identification Through Blind Source Separation. IEEE Signal Processing Letters **13**(2) (2006) 100–103
13. Joho, M., Mathis, H., Lambert, R.H.: Overdetermined blind source separation: Using more sensors than source signals in a noisy mixture. In: Proc. Independent Component Analysis and Blind Signal Separation ICA. (2000) 81–86
14. Bell, A.J., Sejnowski, T.J.: An information maximization approach to blind separation and blind deconvolution. Neural Computation **7**(6) (1995) 1129–1159
15. Delorme, A., Makeig, S.: EEGLAB: an open source toolbox for analysis of single-trial EEG dynamics. Journal of Neuroscience Methods **134** (2004) 9–21
16. Dalal, S.S., Sekihara, K., Nagarajan, S.S.: Modified Beamformers for Coherent Source Region Suppression. IEEE Transactions on Biomedical Engineering (2006) *Accepted for future publication.*
17. Stephens, M.A.: EDF Statistics for Goodness of Fit and Some Comparisons. Journal of the American Statistical Association **69**(347) (1974) 730–737
18. Nagarajan, S.S., Attias, H.T., Hild II, K.E., Sekihara, K.: A graphical model for estimating stimulus-evoked brain responses from magnetoencephalography data with large background brain activity. Neuroimage **30**(2) (2006) 400–416